ARMY RESEARCH LABORATORY

Investigation of Anomalous *n*-Type Behavior in LWIR MBE-Grown $Hg_{1-x}Cd_xTe$ Using Secondary Ion Mass Spectrometry (SIMS)

P. R. Boyd, U. Lee, L. A. Almeida, and J. D. Benson

ARL-TR-701

March 2001

The findings in this report are not to be construed as an official Department of the Army position unless so designated by other authorized documents.

Citation of manufacturer's or trade names does not constitute an official endorsement or approval of the use thereof.

Destroy this report when it is no longer needed. Do not return it to the originator.

Army Research Laboratory

Adelphi, MD 20783-1197

ARL-TR-701 **March 2001**

Investigation of Anomalous *n*-Type Behavior in LWIR MBE-Grown $Hg_{1-x}Cd_xTe$ Using Secondary Ion Mass Spectrometry (SIMS)

P. R. Boyd and U. Lee

Sensors and Electron Devices Directorate, ARL

L. A. Almeida and J. D. Benson

Night Vision and Electronic Sensors Directorate

Abstract

Residual impurities and process-introduced electrically active impurities have long been a source of producibility- and performance-related limitations in $Hg_{1-x}Cd_xTe$ materials and devices. Considerable effort has been expended to reduce the impurity content of II-VI substrate materials and to control the level of both donor and acceptor impurities in thin-film sensing layers. In an effort to develop the next major breakthrough in $Hg_{1-x}Cd_xTe$ materials and device technology, the Communications-Electronics Command (CECOM) Night Vision and Electronic Sensors Directorate (NVESD) has been working on a novel technology tool called the NVESD "microfactory." This MBE-based (molecular beam epitaxy) materials growth and device-fabrication tool is designed to allow for epitaxial materials growth, device fabrication, and passivation processes to be completed in situ in the vacuum system. However, controlled intentional doping of these layers has been hampered by high *n*-type background carrier concentrations in some of the layers after the mercury vacancy anneal. In this work we analyzed a number of MBE $Hg_{1-x}Cd_xTe$ layers, bulk $Cd_{1-Y}Zn_YTe$, and CdTe substrates using secondary ion mass spectrometry (SIMS) to qualitatively determine the major species responsible for the high *n*-type behavior and their possible sources.

Contents

Figures

Tables

1. Introduction

$Hg_{1-x}Cd_xTe$ has become the detector material of choice for most strategic and tactical military infrared imaging applications in the 3- to 5-μm and 8- to 12-μm regions [1]. Residual impurities associated with substrates and source materials, and also process-introduced electrically active impurities have long been a source of producibility- and performance-related limitations for this material system. Considerable effort has been expended to reduce the impurity content of II-VI substrate materials and to control the level of both donor and acceptor impurities in thin-film sensing layers [2]. Many advanced device structures cannot be successfully fabricated at the high growth temperatures required by the current mature liquid-phase epitaxy growth process [3,4]. Hence, a substantial research effort has been under way to develop improved vapor-phase epitaxial growth techniques for II-VI device materials. Infrared focal plane arrays (FPAs) exhibiting a high level of performance have been fabricated from sensing layers grown by both molecular beam epitaxy and metal-organic chemical vapor deposition techniques. In an effort to develop the next major breakthrough in $Hg_{1-x}Cd_xTe$ materials and device technology, the Communications-Electronics Command (CECOM) Night Vision and Electronic Sensors Directorate (NVESD) has been developing a novel technology tool called the NVESD "microfactory" [5,6]. This MBE-based tool is designed to allow for epitaxial materials growth, device fabrication, and passivation processes to be completed in situ in the vacuum system. The quality of MBE $Hg_{1-x}Cd_xTe$ layers grown in the microfactory as demonstrated by etch pit density, double crystal rocking curve, energy dispersive x-ray, and Fourier transform infrared transmission measurements has shown steady improvement. However, controlled intentional doping of these layers has been hampered by high *n*-type background carrier concentrations in some of the layers after the mercury vacancy anneal. Van der Pauw Hall measurements indicated that the background donor concentrations were typically on the order of 10^{18} cm^{-3} for these cases. In this work we analyzed a number of MBE $Hg_{1-x}Cd_xTe$ layers, bulk $Cd_{1-Y}Zn_YTe$, and CdTe substrates using secondary ion mass spectrometry (SIMS) to qualitatively determine the major species responsible for the high *n*-type behavior and their possible sources.

2. Experimental Detail

The MBE $Hg_{1-x}Cd_xTe$ layers were grown in a modified Fisons VG-8 II-VI chamber. Epitaxial $Hg_{1-x}Cd_xTe$ growth was accomplished with Hg, CdTe, and Te cells. The mercury, cadmium, and tellurium fluxes were 2.3 by 10^{-4}, 2.8 by 10^{-6}, and 2.9 by 10^{-6} Torr, respectively. The substrate was independently heated to 180 °C as measured by optical temperature correlation techniques. The $Hg_{1-x}Cd_xTe$ layers were grown on 1.5 by 1.5 cm, <211>B commercially available bulk cadmium zinc telluride ($Cd_{1-Y}Zn_YTe$) substrates. The growth rate was approximately 1.5 μm per hour. Buffer layers were not grown on the $Cd_{1-Y}Zn_YTe$ substrates prior to the initiation of $Hg_{1-x}Cd_xTe$ growth.

SIMS measurements were taken with an Atomika 3000-30 Ionprobe A-DIDA.* Depth profiles were made with oxygen at 6-, 9-, and 12-keV primary ion energies. The primary ion gun was equipped with an oxygen cold cathode source. A better signal-to-noise ratio (SNR) and a higher negative ion yield could be obtained with a cesium ion gun; however, a cesium source was not available on our system during this work. With the oxygen source, it was still possible to get signal count rates that were three orders of magnitude higher than the background noise level. Table 1 shows a typical set of instrumental operating parameters.

Table 1. Typical data acquisition parameters for the chlorine-35 profiles.

Primary ions:	Oxygen
Ion energy:	6 keV
Beam current:	100 nA
Scan width:	0.200 mm
Scan speed:	2 s/frame
Scan gate:	30%

*Atomika Analysetechnik GmbH, Bruckmannring 6, W-8042 Oberschleissheim, München, Germany.

3. Results and Discussion

Verified *n*-type dopants in $Hg_{1-x}Cd_xTe$ [7,8,9] are shown in table 2. The initial motivation to study the chlorine content in the epitaxial layers was based on the results of in situ Auger analysis of a number of these layers. The Auger analysis indicated that the surfaces were characterized by very high chlorine concentrations. Although it is common to observe chlorine contamination on semiconductor surfaces exposed to the ambient environment, the large chlorine Auger signals obtained from these sample surfaces clearly indicated that a more detailed analysis of the chlorine distribution in these materials was required. Chlorine situated on a tellurium site in $Hg_{1-x}Cd_xTe$ is an *n*-type dopant [7–9]. Marais and Botha et al [10,11] also showed that chlorine in solid state recrystallized $Hg_{1-x}Cd_xTe$ exhibits donor behavior at varying activation levels. Over the concentration range of 1×10^{17} cm^{-3} to 4×10^{14} cm^{-3}, the activation level is a function of its concentration in the crystal. Faurie et al [12] demonstrated that impurity diffusion from bulk, commercial CdZnTe substrates can play a major role in the electrical properties of HgCdTe IR sensing layers grown by molecular beam epitaxy on these substrates.

Table 2. *n*-type dopants in $Hg_{1-x}Cd_xTe$

Impurity (site)	Major isotopes		
Zn (i)	64	66	68
Hg (i)	202	200	199
B (m)	11	10	—
Al (m)	27	—	—
Ga (m)	69	71	—
In (m)	115	113	—
Si (m)	28	29	30
Ge (m)	74	72	70
Sn (m)	120	118	116
Pb (m)	208	206	207
O (i)	16	17	18
F (Te)	19	—	—
Cl (Te)	35	37	—
Br (Te)	79	81	—
I (Te)	127	—	—
Fe (Te)	56	64	57
Ni (Te)	58	60	62
Ti (m)	48	46	47
C (m)	12	13	14

We identified the SIMS mass 35 negative ion as chlorine by confirming the correct isotopic ratio from the ion intensity data collected at mass 35 and mass 37. Figure 1 shows the SIMS mass 35 negative ion depth profile for the NVESD MBE sample number 0706. In this case we also profiled and monitored the mercury positive ion at mass 202, and overlaid the two profiles to determine where the interface between the $Hg_{1-x}Cd_xTe$ epilayer and the $Cd_{1-Y}Zn_YTe$ substrate was positioned. A spike in the chlorine ion concentration can be observed at the top surface of the $Hg_{1-x}Cd_xTe$ epilayer and also at the $Hg_{1-x}Cd_xTe/Cd_{1-Y}Zn_YTe$ interface. The chlorine ion signal intensity after the initial surface spike remains fairly constant throughout the entire 6-μm MBE $Hg_{1-x}Cd_xTe$ layer and into the underlying $Cd_{1-Y}Zn_YTe$ substrate. The intensity of the chlorine ion at mass 35 appears slightly higher in the epitaxial layer than in the substrate. This may be related to the ion yield, surface potential changes, or collection efficiency issues rather than an actual change in the concentration of the chlorine impurity. As a reference sample, we next profiled a clean silicon wafer to eliminate system contamination and other artifacts as possible explanations for the high chlorine levels observed in the MBE $Hg_{1-x}Cd_xTe$ layers. The Cl-35 depth profile of the silicon wafer exhibited the expected surface concentration spike, followed,

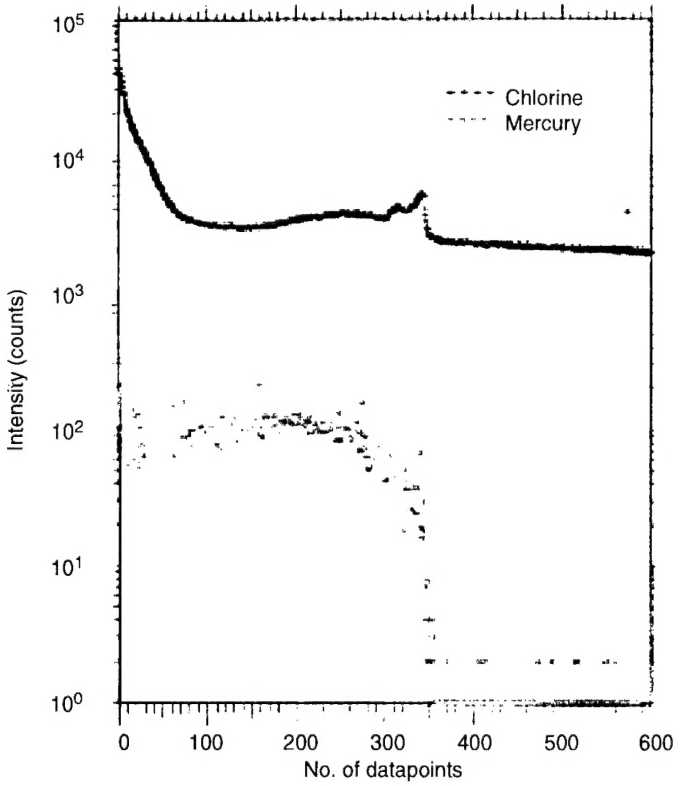

Primary ions: Oxygen
Ion energy: 6 (keV)
Beam current: 100 (nA)
Scan width: 0.200 (mm)
Scan speed: 2 (s/frame)
Scan gate: 30 (%)

Label	Mass	Cycles	Energy
Chlorine	35.0	10	15.0
Mercury	202.0	10	−20.0

Figure 1. SIMS mass 35 negative ion depth profile overlaid on mercury positive ion mass 202 depth profile for NVESD MBE sample number 0706.

after several sweeps, by a rapid decrease to the background noise level. In an effort to determine the source(s) of the chlorine contamination, we analyzed a number of $Cd_{1-Y}Zn_YTe$ and CdTe substrates and process-related materials.

One method of mounting the samples to the molybdenum block in the MBE system involved the use of commercial aquadag or colloidal graphite conductive adhesives. We acquired a Cl-35 SIMS (fig. 2) profile for the adhesive mounted on a silicon wafer. This tended to indicate that the colloidal graphite adhesive was a major source of chlorine contamination in the MBE layers. When we modified the sample-mounting procedure to a gallium-based process, the SIMS mass 35 depth profile exhibited a dramatically reduced chlorine ion intensity (fig. 3). The Hall data obtained from these subsequent $Hg_{1-x}Cd_xTe$ layers indicated that the *n*-type carrier concentration had been reduced from approximately 10^{18} cm^{-3} to the mid- to low-10^{15} cm^{-3} range. However, some of the subsequent MBE $Hg_{1-x}Cd_xTe/Cd_{1-Y}Zn_YTe$ structures still exhibited Cl-35 signatures in the epitaxial layers and substrates. We then analyzed a number of commercial $Cd_{1-Y}Zn_YTe$ substrates. We acquired depth profiles from substrates from different commercial sources. In agreement with the work of Faurie et al [12] and Wijewarnasuriya et al [13,14],

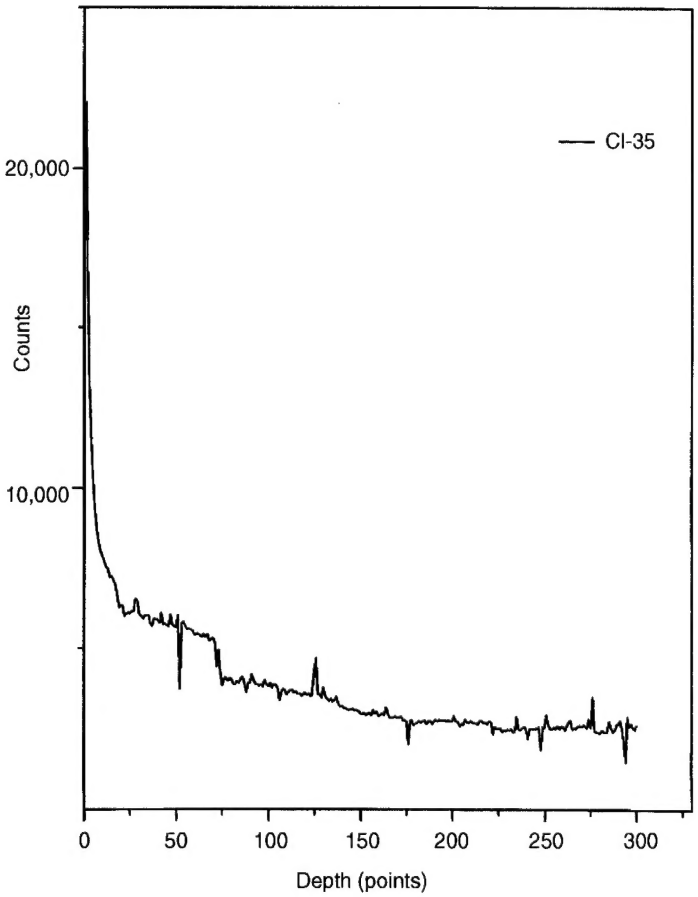

Figure 2. Chlorine mass 35 SIMS depth profile of a commercial colloidal graphite used as an adhesive to attach II-VI substrates to mounting block in MBE machine.

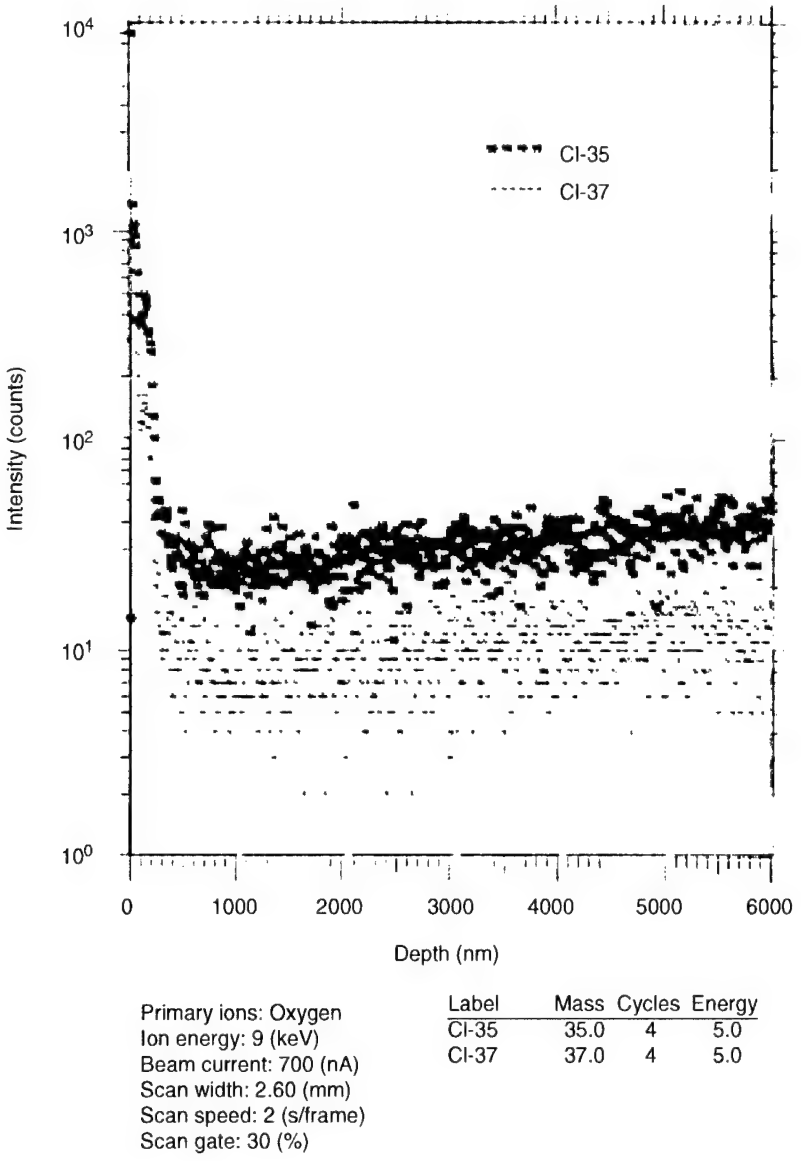

Figure 3. SIMS mass 35 depth profile of an MBE-grown $Hg_{1-x}Cd_xTe$ layer acquired after replacing colloidal graphite adhesive with gallium.

the chlorine levels in the commercial substrates from different vendors varied widely. Figure 4 shows an example of a commercial $Cd_{1-Y}Zn_YTe$ substrate with a high chlorine background-impurity level. Figure 5 shows a SIMS profile of a commercial CdTe substrate exhibiting noise-level bulk Cl-35 intensity. The data clearly indicate that the commercial $Cd_{1-Y}Zn_YTe$ substrates can have significantly different concentrations of chlorine and/or other electrically active impurities that can negatively impact the viability of these substrates for reproducible device-quality $Hg_{1-x}Cd_xTe$ epitaxial layer growth. Several of these contaminated epitaxial layers were analyzed with a Cameca 4F at an industrial laboratory. Indicated chlorine concentrations, based on the relative sensitivity factors for the Cameca, were on the order of 10^{18} cm^{-3}, which was in good agreement with the results of the Hall measurements.

Figure 4. Example of mass 35 SIMS depth profile of a commercial $Cd_{1-Y}Zn_YTe$ substrate characterized with a high chlorine background impurity level.

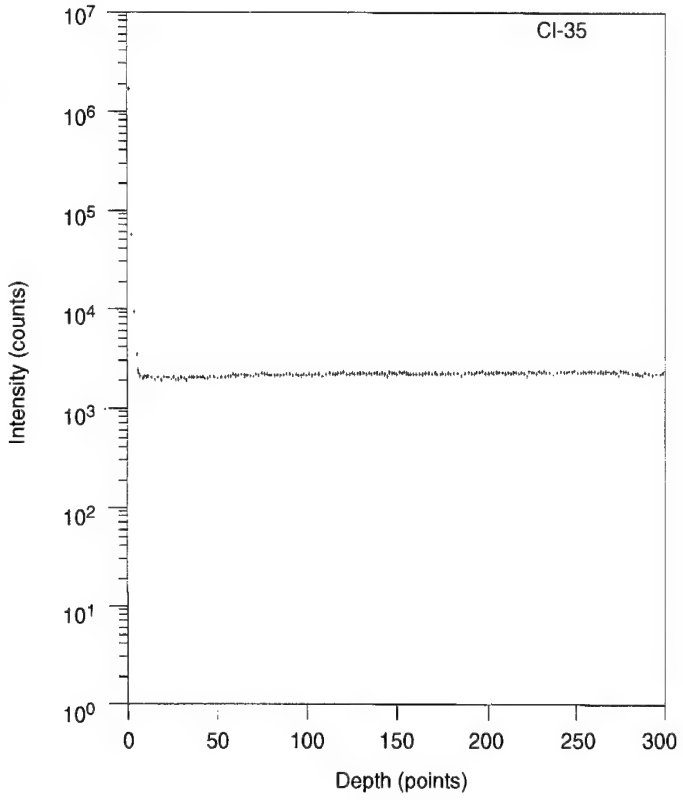

Figure 5. SIMS depth profile of a commercial CdTe substrate exhibiting noise-level bulk Cl-35 intensity.

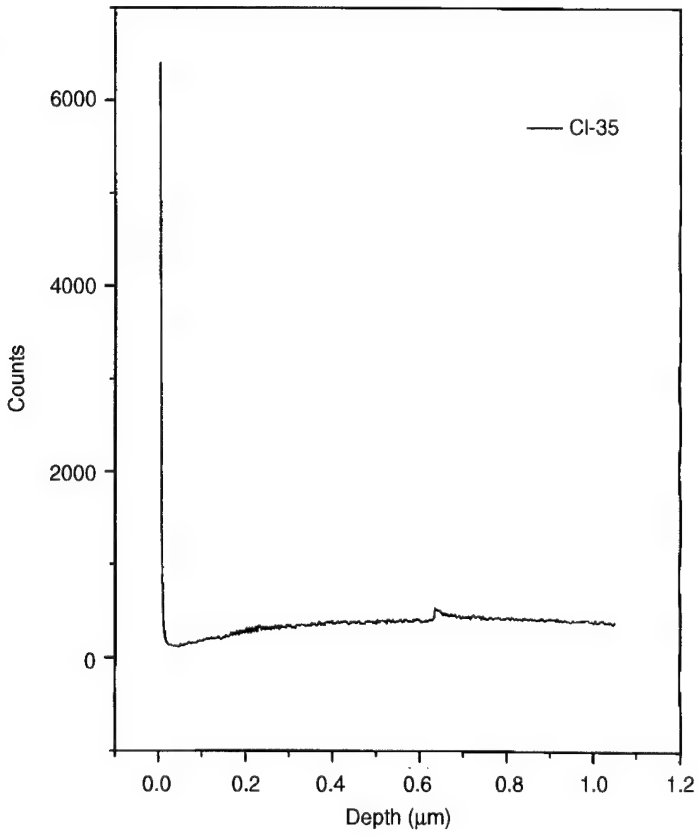

When NVESD initiated doping experiments in the microfactory, control of the *n*-type carrier concentration again became an issue. Mixed conduction, which becomes more of an issue at lower carrier concentrations, was not a factor in these samples because the *n*-type carrier concentration was in the 10^{18} cm^{-3} range. Control of the indium concentration in these layers could not be accomplished through control of the indium effusion cell temperature. To determine the source of the indium background, a 12.6-µm-thick MBE $Hg_{1-x}Cd_xTe$ layer, sample number 022500, was grown on a bulk $Cd_{1-Y}Zn_YTe$ substrate. The growth run was terminated with a 350-Å layer of CdTe. The epitaxial layer consisted of three distinct steps. A 4-µm nominal $x = 0.51$ layer was grown first. Then the CdTe effusion cell temperature was increased and a 3.2-µm $x = 0.62$ layer was grown. In step three, the Te effusion cell temperature was increased again and a 5.4-µm layer with an x-value of 0.52 was deposited. Figure 6 shows the positive ion depth profile of this film. The intensity of the indium-115 ion shows a sharp increase between steps 1 and 2. At the step 2 to 3 transition, the indium ion intensity returns to the general level associated with step 1. The SIMS analysis clearly indicated that the CdTe effusion cell was the source of the uncontrolled indium

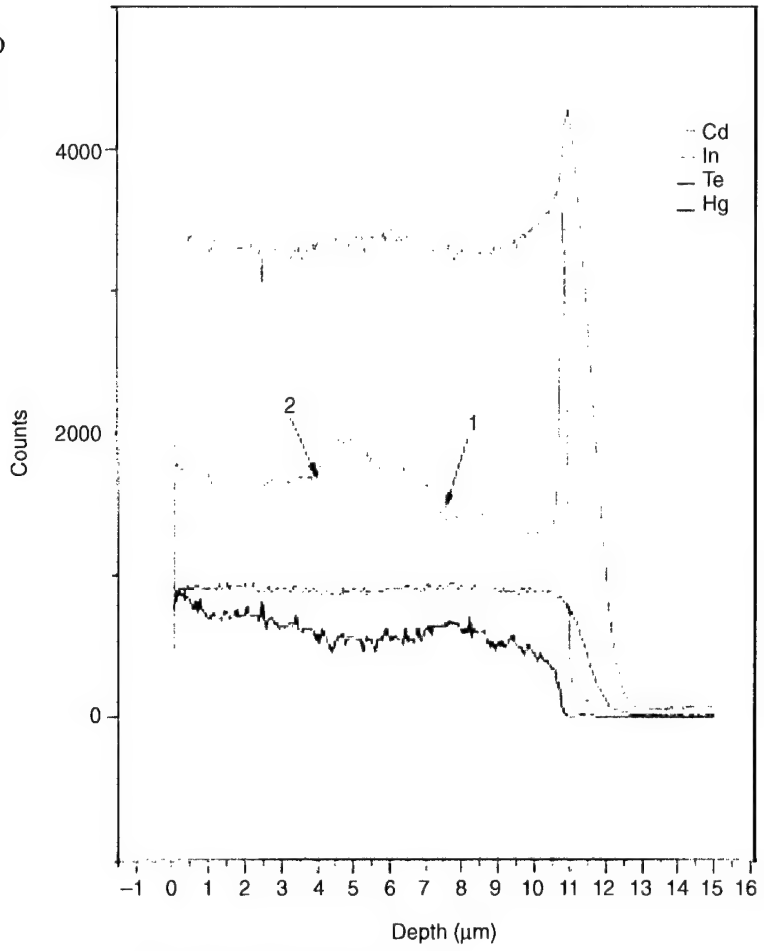

Figure 6. Positive ion depth profile of NVESD MBE $Hg_{1-x}Cd_xTe$ sample number 022500.

1. Increased CdTe cell temperature
2. Increased Te cell temperature

doping of these layers. MBE $Hg_{1-x}Cd_xTe$ layers exhibiting *n*-type carrier concentrations in the low 10^{15} cm^{-3} range were obtained when a new CdTe effusion cell was incorporated into the microfactory system, and the configuration of the effusion cells in the MBE system was modified.

In conclusion, we applied SIMS analysis to a series of CdTe and $Cd_{1-Y}Zn_YTe$ substrates and MBE $Hg_{1-x}Cd_xTe$ layers to determine the identity and source of high *n*-type carrier concentrations in epitaxial layers grown in a novel $Hg_{1-x}Cd_xTe$ materials growth and device-fabrication tool being developed at the NVESD. We determined chlorine to be a major contributor to the *n*-type behavior and identified mounting procedures and substrates with high chlorine impurity levels as the major sources of contamination. We also established the root cause of the lack of control in the indium doping process in the microfactory system.

References

1. Reine, M. B., A. K. Sood, and T. J. Tredwell, *Semiconductors and Semimetals*, R. K. Willardson and A. C. Beer, eds., **18** (1981), 201–305.
2. Dean, B. E., C. J. Johnson, and F. J., Kramer, *J. Cryst. Growth* **106** (1990), 47–50.
3. Chu, M., S. Terterian, H. K. Gurgenian, Y. Z. Liu, C. C. Wang, and J. J. Kennedy, Proc. SPIE **2228** (1994), 194–200.
4. Neugebauer, G. T., R. Shetty, C. K. Ard, and P. W. Norton, Proc. SPIE **2228** (1994), 2–11.
5. Dinan, J. H., J. D. Benson, A. B. Cornfeld, M. Martinka, J. N. Johnson, J. Bratton, and P. Taylor, Proc. 1996 IEEE-CPMT International Electronic Manufacturing Technology Symposium, Austin, TX (October 1996).
6. Almeida, L. A., J. N. Johnson, J. D. Benson, J. H. Dinan, and B. Josh, *J. Electron. Mater.* **27** (1998), 500.
7. Capper, P., *J. Cryst. Growth* **57** (1982), 280–299.
8. Capper, P., *J Vac. Sci. Technol.* **B9**, 3 (1991), 1667–1681.
9. Astles, M. G., G. Blakemore, S. Courtney, and N. Shaw, *J. Cryst. Growth* **91** (1988), 1–10.
10. Marais, M. A., H. J. Strydom, J. H. Basson, D.E.C. Rogers, and H. Booyens, *J. Cryst. Growth* **88** (1988), 391.
11. Botha, A. P., H. J. Strydom, and M. A. Marais, *Nucl. Instrum. Methods* **B35** (1988), 420.
12. Faurie, J. P., S. Sivananthan, and P. S. Wijewarnasuriya, Proc. SPIE **1735** (1992), 141.
13. Wijewarnasuriya, P. S., M. D. Lange, S. Sivananthan, and J. P. Faurie, *J. Electron. Mater.* **24**, 9 (1995).
14. Wijewarnasuriya, P. S., J. P. Faurie, and S. Sivananthan, *J. Cryst. Growth* **159** (1996), 1136–1140.

Distribution

Admnstr
Defns Techl Info Ctr
ATTN DTIC-OCP
8725 John J Kingman Rd Ste 0944
FT Belvoir VA 22060-6218

DARPA
ATTN S Welby
3701 N Fairfax Dr
Arlington VA 22203-1714

Ofc of the Secy of Defns
ATTN ODDRE (R&AT)
The Pentagon
Washington DC 20301-3080

Ofc of the Secy of Defns
ATTN OUSD(A&T)/ODDR&E(R) R J Trew
3080 Defense Pentagon
Washington DC 20301-7100

AMCOM MRDEC
ATTN AMSMI-RD W C McCorkle
Redstone Arsenal AL 35898-5240

US Army TRADOC
Battle Lab Integration & Techl Directrt
ATTN ATCD-B
FT Monroe VA 23651-5850

BMDO Direct, Engrg Conc & Compon
ATTN TOR J Pohlmann
1725 Jefferson Davis Highway Ste 809
Arlington VA 22202-4102

US Military Acdmy
Dept of Mathematical Sci
ATTN MAJ L G Eggen
West Point NY 10996-1786

US Military Acdmy
Mathematical Sci Ctr of Excellence
ATTN MADN-MATH MAJ M Huber
Thayer Hall
West Point NY 10996-1786

NVESD
ATTN AMSEL-RD-NV D Benson
ATTN AMSEL-RD-NV J Ratches
10221 Burbeck Rd Ste 430
FT Belvoir VA 22060-5806

Dir for MANPRINT
Ofc of the Deputy Chief of Staff for Prsnnl
ATTN J Hiller
The Pentagon Rm 2C733
Washington DC 20301-0300

SMC/CZA
2435 Vela Way Ste 1613
El Segundo CA 90245-5500

TECOM
ATTN AMSTE-CL
Aberdeen Proving Ground MD 21005-5057

US Army ARDEC
ATTN AMSTA-AR-TD
Bldg 1
Picatinny Arsenal NJ 07806-5000

Director
US Army CECOM RDEC
FT Monmouth NJ 07703-5201

US Army Info Sys Engrg Cmnd
ATTN AMSEL-IE-TD F Jenia
FT Huachuca AZ 85613-5300

Distribution (cont'd)

US Army Natick RDEC
ATTN SSCNC-T
Natick MA 01760-5002

US Army Natick RDEC Acting Techl Dir
ATTN SBCN-T P Brandler
Natick MA 01760-5002

US Army Simulation Train & Instrmntn Cmnd
ATTN AMSTI-CG M Macedonia
ATTN J Stahl
12350 Research Parkway
Orlando FL 32826-3726

US Army Soldier & Biol Chem Cmnd Dir of Rsrch & Techlgy Directrt
ATTN SMCCR-RS I G Resnick
Aberdeen Proving Ground MD 21010-5423

US Army Tank-Automtv Cmnd RDEC
ATTN AMSTA-TR J Chapin
Warren MI 48397-5000

Nav Surfc Warfare Ctr
ATTN Code B07 J Pennella
17320 Dahlgren Rd Bldg 1470 Rm 1101
Dahlgren VA 22448-5100

Hicks & Assoc Inc
ATTN G Singley III
1710 Goodrich Dr Ste 1300
McLean VA 22102

Palisades Inst for Rsrch Svc Inc
ATTN E Carr
1745 Jefferson Davis Hwy Ste 500
Arlington VA 22202-3402

Director
US Army Rsrch Ofc
ATTN AMSRL-RO-D JCI Chang
ATTN AMSRL-RO-EN W D Bach
PO Box 12211
Research Triangle Park NC 27709

US Army Rsrch Lab
ATTN AMSRL-CI-AI-R Mail & Records Mgmt
ATTN AMSRL-CI-AP Techl Pub (2 copies)
ATTN AMSRL-CI-LL Techl Lib (2 copies)
ATTN AMSRL-D D R Smith
ATTN AMSRL-DD J M Miller
ATTN AMSRL-SE-E H Pollehn
ATTN AMSRL-SE-E W Clark
ATTN AMSRL-SE-EM J Pamulapati
ATTN AMSRL-SE-EM P Boyd (25 copies)
Adelphiw MD 20783-1197

REPORT DOCUMENTATION PAGE

Form Approved
OMB No. 0704-0188

1. AGENCY USE ONLY *(Leave blank)*	2. REPORT DATE	3. REPORT TYPE AND DATES COVERED
	March 2001	Summary, Oct 98–Sep 99

4. TITLE AND SUBTITLE Investigation of Anomalous *n*-Type Behavior in LWIR MBE-Grown $Hg_{1-x}Cd_xTe$ Using Secondary Ion Mass Spectrometry (SIMS)

5. FUNDING NUMBERS
DA PR: A31B
PE: 61102A

6. AUTHOR(S) P. R. Boyd and U. Lee (ARL), L. A. Almeida and J. D. Benson (Night Vision and Electronic Sensors Directorate)

7. PERFORMING ORGANIZATION NAME(S) AND ADDRESS(ES)
U.S. Army Research Laboratory
Attn: AMSRL-SE-EI email: prboyd@arl.army.mil
2800 Powder Mill Road
Adelphi, MD 20783-1197

8. PERFORMING ORGANIZATION REPORT NUMBER
ARL-TR-701

9. SPONSORING/MONITORING AGENCY NAME(S) AND ADDRESS(ES)
U.S. Army Research Laboratory
2800 Powder Mill Road
Adelphi, MD 20783-1197

10. SPONSORING/MONITORING AGENCY REPORT NUMBER

11. SUPPLEMENTARY NOTES
ARL PR: 9NE1BB
AMS code: 611102.31B

12a. DISTRIBUTION/AVAILABILITY STATEMENT Approved for public release; distribution unlimited.

12b. DISTRIBUTION CODE

13. ABSTRACT *(Maximum 200 words)*

Residual impurities and process-introduced electrically active impurities have long been a source of producibility- and performance-related limitations in $Hg_{1-x}Cd_xTe$ materials and devices. Considerable effort has been expended to reduce the impurity content of II-VI substrate materials and to control the level of both donor and acceptor impurities in thin-film sensing layers. In an effort to develop the next major breakthrough in $Hg_{1-x}Cd_xTe$ materials and device technology, the Communications-Electronics Command (CECOM) Night Vision and Electronic Sensors Directorate (NVESD) has been working on a novel technology tool called the NVESD "microfactory." This MBE-based (molecular beam epitaxy) materials growth and device-fabrication tool is designed to allow for epitaxial materials growth, device fabrication, and passivation processes to be completed in situ in the vacuum system. However, controlled intentional doping of these layers has been hampered by high *n*-type background carrier concentrations in some of the layers after the mercury vacancy anneal. In this work we analyzed a number of MBE $Hg_{1-x}Cd_xTe$ layers, bulk $Cd_{1-Y}Zn_YTe$, and CdTe substrates using secondary ion mass spectrometry (SIMS) to qualitatively determine the major species responsible for the high *n*-type behavior and their possible sources.

14. SUBJECT TERMS	15. NUMBER OF PAGES
Detector materials, impurity analysis, II-VI material substrates	17
	16. PRICE CODE

17. SECURITY CLASSIFICATION OF REPORT	18. SECURITY CLASSIFICATION OF THIS PAGE	19. SECURITY CLASSIFICATION OF ABSTRACT	20. LIMITATION OF ABSTRACT
Unclassified	Unclassified	Unclassified	UL

NSN 7540-01-280-5500

Standard Form 298 (Rev. 2-89)
Prescribed by ANSI Std. Z39-18
298-102